

Do Dynamical Excitonic Liquid Correlations Mediate Superconductivity in Elemental Bismuth?

S. Koley^{3,*}, M. S. Laad^{1,†} and A. Taraphder^{2‡}

¹*Instt. Math. Sciences Taramani, Chennai, 600113 and Homi Bhabha National Institute, India*

²*Department of Physics and Centre for Theoretical Studies,
Indian Institute of Technology, Kharagpur, 721302 India and*

³*Department of Physics, St. Anthony's College, Shillong, Meghalaya, 793001 India*

Motivated by the remarkable discovery of superconductivity in elemental Bismuth, we study its normal state in detail using a combination of tight-binding (TB) band-structural supplemented by dynamical mean-field theory (DMFT). We show that a two-fluid model composed of preformed and dynamically fluctuating excitons coupled to a tiny number of carriers provides a unified rationalization of a range of ill-understood normal state spectral and transport data. Based on these, we propose that resonant scattering involving a very low density of renormalized carriers and the excitonic liquid drives logarithmic enhancement of vertex corrections, boosting superconductivity in *Bi*. A confirmatory test for our proposal would be the experimental verification of an excitonic semiconductor with electronic nematicity as a ‘competing order’ on inducing a semi-metal-to semiconductor transition in *Bi* by an external perturbation like pressure.

PACS numbers: 25.40.Fq, 71.10.Hf, 74.70.-b, 63.20.Dj, 63.20.Ls, 74.72.-h, 74.25.Ha, 76.60.-k, 74.20.Rp

Rhombohedral Bismuth (Bi) has recently acquired prominence in a variety of contexts. Like graphite, elemental Bi also shows a magnetic field- as well as a pressure-induced metal-insulator-like transition¹ with a large magneto-resistance, and electron fractionalization in high magnetic fields². Remarkable discovery of superconductivity (SC) in Bi at very low temperature ($T_c \simeq 0.5$ mK)³ in a lowest carrier elemental system to date adds to the range of novel behaviors exhibited by this ‘simple’ system. Experiments conclusively establish that SC in Bi is *not* of the standard BCS variety and, in fact, it would be more aptly characterized as being in a non-adiabatic limit of pairing theory if electron-phonon coupling were to be invoked as the dominant pairing glue.

The unique electronic properties of *Bi* arise from successive distortions of a higher-symmetry simple-cubic structure. First, a small relative displacement along the body diagonal doubles the unit cell. By itself, this would drive *Bi* into a Peierls-like band semiconductor. But additional rhombohedral shear causes further lowering of symmetry, allowing valence and conduction band overlap - in good accord with band structure studies, and explains why *Bi* is metallic. Due to extremely small Fermi pockets (of size 10^{-5} of the Brillouin zone) and tiny carrier density ($3 \times 10^{17} \text{cm}^{-3}$), the long mean-free path accounts for its small low- T resistivity. One might then think that traditional one-electron band structure is an adequate framework to understand its electronic properties.

However, careful perusal of extant data points toward a much more interesting situation. Early data⁹ show that the electrical resistivity $\rho_{dc}(T) \simeq \rho_0 + AT^2$ for $T < 50$ K. But very unusual behavior at low T , with $\rho_{dc}(T) \simeq T^5$ was recently seen that invoked a plasmaron picture⁴. Optical data raise additional issues in this context⁵. While a tiny Drude component is visible at low energy, finding of sizable mid-infra-red (mid-IR) absorption is inexplicable in a free-electron framework. Given the tiny Fermi

energy $\simeq 25$ meV, a large T -dependent transfer of spectral weight over a much larger scale $\simeq 300$ meV also presents a challenge for the standard (uncorrelated band) view. On the theoretical front, first-principles density-functional theory (DFT) and Slater-Koster tight-binding fits⁶ conclusively show that: (*i*) there are multiple tiny pockets in *Bi*, with two being almost perfectly compensated, and the others supplying a tiny additional number of carriers. Moreover, the importance of spin-orbit coupling (SOC) is shown by the fact that the correct positions of the e(h) pockets are only found when SOC is included in band calculations. While DFT+SOC calculations indeed yield the correct shape and size of the carrier pockets, they cannot, by construction, rationalize the above features. It is long known⁵ that the dominant interaction between conduction and valence band carriers in *Bi* is of short-range excitonic character, but its role in *Bi* has never been satisfactorily addressed. Generically, one also expects a symmetry-adapted coupling of such interband exciton-like entities to intervalley phonons⁷. As far as SC is concerned, the large discrepancy³ between the measured and calculated (within BCS theory) ratio of the upper critical field to T_c also indicates a non-adiabatic ‘strong coupling’ SC. These limited observations must constrain theoretical modelling: both unconventional metallicity and SC must find explication in a picture based on (*i*) the special band structure of Bi and (*ii*) strong scattering (electron-hole and/or electron-phonon) processes beyond DFT and, in particular, microscopic processes which generate a $\rho_{dc} \simeq T^5$ should also be involved in generating the SC pair glue.

Our first observation is that two of the multiple electron(hole) pockets of Bi are almost perfectly compensated, leading to a situation famously encountered in transition-metal dichalcogenides (TMD), where preformed excitonic liquid (PEL) driven charge-density-wave (CDW) states are ubiquitous^{8,10}. Band calculations

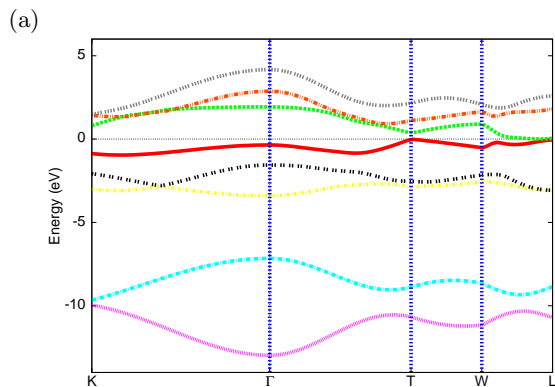


FIG. 1. (Color Online) Tight binding (TB) bands of Bi in the rhombohedral structure including spin-orbit coupling (SOC) as done in Ref.⁶. For the effective two-band model incorporating excitonic correlations within DMFT calculations, we use only the two (red and green) bands crossing the Fermi energy, $E_F (= 0)$.

reveal a total of four pockets in Bi , of which two (electron and hole) exhibit a propensity for an excitonic instability. Were there only these two pockets, one would have expected an electron-hole attraction-mediated excitonic insulator. However, the remaining pockets now supply a tiny number of additional carriers, leading to a physical picture of *an incipient excitonic insulator self-doped with a tiny number of carriers*. Implicit herein is the fact that poor screening of the interband Coulomb interaction due to ultra-low carrier density makes this a strongly interacting system. Thus, we are led to a model of a self-doped excitonic insulator (EI) in the intermediate coupling limit, where novel physics can arise from strong scattering between carriers and preformed but uncondensed excitons. In this letter, we establish this using tight-binding-plus dynamical mean-field theory (TB-DMFT) calculations as done earlier^{8,10}. Having good accord with normal state transport, we elucidate a ‘strong coupling’ electronic mechanism, wherein strong resonant scattering between carriers and preformed excitons enhances the SC T_c .

We begin by using the Slater-Koster (SK) fit with form factors and parameters *including* SOC as in earlier work⁶. The resulting band structure in Fig. 1 excellently reproduces all the pockets seen in full DFT calculations, constituting the appropriate band structural input for the correlation calculations. Guided by the discussion above, we focus on inter-band excitonic correlations. The two-band Hubbard model incorporating the two bands crossing the Fermi energy is $H = H_0 + H_1$, with

$$H_0 = \sum_{(\mu,\nu=1,2),k,\sigma} \epsilon_\mu(k) c_{k\mu\sigma}^\dagger c_{k\nu\sigma} + h.c. + \Delta \sum_i (n_{i,1} - n_{i,2}) \quad (1)$$

where $\epsilon_1(k) = E_p + 3V_{pp\pi} \cos(\frac{\sqrt{3}k_x}{2}) \cos(\frac{k_y}{2}) + V_{pp\pi} [\cos(\frac{\sqrt{3}k_x}{2}) \cos(\frac{k_y}{2}) + 2\cos k_y]$ (represented by the green line in Fig. 1), $\epsilon_2(k) = E_p + V_{pp\sigma} [\cos(\frac{\sqrt{3}k_x}{2}) \cos(\frac{k_y}{2}) +$

$2\cos k_y] + 3V_{pp\pi} \cos(\frac{\sqrt{3}k_x}{2}) \cos(\frac{k_y}{2})$ (red line in Fig. 1) where E_p is on-site energy, $V_{pp\pi}$ and $V_{pp\sigma}$ are third nearest neighbour interaction and the interband matrix element $V_{12}(k) \simeq 2i\sqrt{3}\sin(\frac{\sqrt{3}k_x}{2})\sin(\frac{k_y}{2})$, as extracted earlier⁶ from an SK fit. Here μ, ν represent the band indices for the two bands crossing $E_F (= 0)$ in Fig. 1. The local terms are

$$H_1 = \sum_{\mu=1,2} U_{\mu\mu} \sum_i n_{i\mu\uparrow} n_{i\mu\downarrow} + U' \sum_i n_{i,1} n_{i,2} \quad (2)$$

Since $g = \omega_D/E_F \simeq 0.5$ (g =electron-phonon coupling, E_F =Fermi energy) is actually sizable in Bi^3 , one is in a non-adiabatic limit. In contrast to the anti-adiabatic ($g \rightarrow \infty$) or the adiabatic ($g \rightarrow 0$) limits, one cannot ‘integrate out’ the (intervalley in Bi) phonons to give a further e-h attraction $O(g^2/\hbar\omega_D)$. One must solve H including an explicit $e-p$ term by coupling the intervalley phonons to the \mathbf{k} -dependent hybridization as done in earlier work¹⁰.

TB+DMFT Results and Transport

We solve the two-band model above using DMFT, with multi-orbital IPT as the ‘impurity’ solver. Though not numerically exact, it works very well in real multi-band cases where there is a considerable crystal-field splitting between the bands (here, between valence and conduction band). It is a fast solver and its efficacy in a wide range of real systems is known^{10,11}. In contrast, though QMC solvers are much more reliable, they cannot access temperatures below $O(20)$ K at present, which makes them unsuitable for investigation of the low $T (< 10$ K) states. We choose $U = 0.5 - 0.7$ eV and $U' = 0.1 - 0.2$ eV as appropriate parameters, and while ab-initio estimates will yield more precise estimates, our present choice is physically motivated. Given widths of $O(1.0 - 1.5)$ eV for the valence (VB) and conduction (CB) bands, we are in the intermediate coupling limit of the two-band model. This is precisely the case where DMFT works best (for specific studies in the BCS-BEC crossover, see¹²).

In Fig. 2, we show the TB+DMFT local density-of-states (LDOS) as U, U' are cranked up. While correlations gradually close the band gap for the VB (‘ a ’-orbital) as expected¹³, they reduce the LDOS at E_F for the CB (‘ b ’ orbital): these contrasting behaviors are direct consequences of distinct effects of local electronic correlations on band-insulating and metallic subsets of the non-interacting band structure. Around $U \simeq W_b$, the b -fermion band-width, we observe eventual opening of a *Mott*-like gap in the LDOS, seen by the fact that $\text{Im}\Sigma_b(\omega)$ develops a pole structure at E_F in this case. Correspondingly, the a -fermion states retain metallic character: this would be an interesting manifestation of orbital-selective Mott physics in semi-metals and, were such a strong coupling regime to be realized, would open up the possibility to development of novel instabilities with concomitant competing orders¹⁴ as, for instance, in Fe-arsenides.

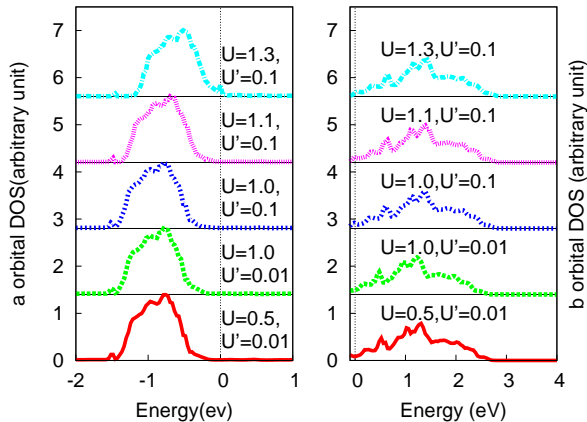


FIG. 2. (Color Online) The orbitaly resolved density of states from TB+DMFT at various U and U' .

However, this is *not* the regime applicable to *Bi*, and so we concentrate on the smaller U regime. Choosing $U = 0.5$ eV, $U' = 0.15$ eV, we next compute the *dc* resistivity using the Kubo formalism in DMFT. This task is facilitated by the finding¹⁵ that irreducible vertex corrections appearing the Bethe-Salpeter equations for conductivities are negligible and can be ignored to a very good approximation. Interestingly, as shown in Fig. 3, we find that a linear-in- T behavior of $\rho_{dc}(T)$ at ‘high’ $T \geq 40 - 50$ K smoothly crosses over to a Fermi-liquid-like T^2 behavior up to about 10 K and, remarkably, exhibits a further low- T crossover to a ‘good’ metal with $\rho_{dc}(T) \simeq T^5$. This is in very good accord with experimental trends, and mandates deeper microscopic rationalization. To cement the link between transport and excitonic liquid fluctuations, Fig. 3 shows the *excitonic* average, computed as $\Delta_{exc} = (-1/\pi) \int d\omega \text{Im}G_{12}(\omega)$ ($G_{12}(\omega)$ is itself computed from two-band DMFT(IPT) as previously done for TMDs¹⁰). We find a clear correlation between $\Delta_{exc}(T)$ and the T -dependence of $\rho_{dc}(T)$ over a wide T range. This provides strong theoretical evidence linking (at least) the *dc* resistivity to microscopic processes involving scattering of the tiny number of carriers off well-formed and quasi-local excitonic correlations: at high- T , the latter are incoherent, leading to a quasi-linear-in- T resistivity, while increasing one-fermion coherence via suppression of incoherent excitonic fluctuations provides a rationalization for the near T^2 at intermediate T . Remarkably, however, we also obtain the $\rho_{dc}(T) \simeq T^5$ dependence at very low T , the latter correlated with a reduced excitonic fluctuation at low T . Thus, we identify a new element: the T -dependence of sizable and dynamical ‘preformed’ excitonic correlations governs the T -dependent resistivity in a wide T window. Our proposal is distinct from: (i) the plasmaron view⁴, where weak-coupling RPA-like analysis, based upon a picture of efficient screening, is employed to get $\rho_{dc} \simeq T^5$ from long-range interactions, and (ii) pure e-p coupling models, which could, in principle, also yield

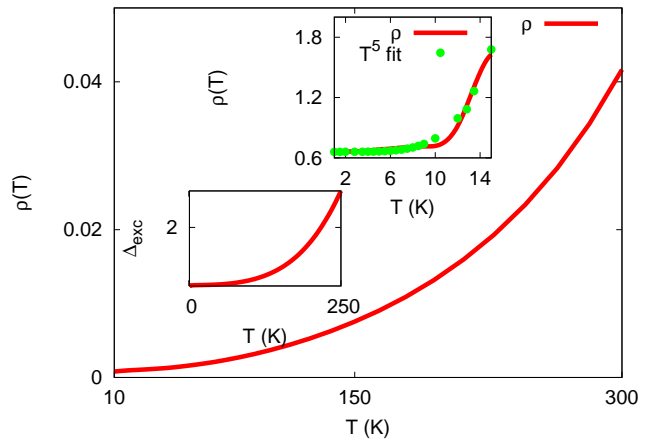


FIG. 3. (Color Online) *DC* Resistivity for *Bi* within TB+DMFT: a T -dependent crossover from $\rho_{dc}(T) \simeq T$ at ‘high’- T to a correlated Landau-Fermi liquid like $\rho_{dc}(T) \simeq T^2$ below $T \simeq 90$ K is followed by $\rho_{dc}(T) \simeq T^5$ form at very low T (see inset for comparison with data points) is clear. The lower-left inset shows the T -dependent *local* interband excitonic average: onset of $\rho_{dc}(T) \simeq T^5$ correlates with a decreasing excitonic average. The y-axis of both the insets are divided by 10^{-3} .

similar behavior when $T \ll \Theta_D$, something that may also obtain in *Bi*. We propose that a way to distinguish between these distinct scenarios could be T -dependent tunnelling measurements at small-to-intermediate T : as a function of T , the conductance $g(V) = dI/dV$ would, in a picture involving coupling of carriers to any bosonic mode(s), show finite-voltage (energy) peak-dip-hump features. The energies and spectral weights of such features could be compared with estimates from different bosonic channels, allowing a determination of the most important fermion-boson scattering channel. However, since there will always be a symmetry-dictated coupling of interband excitons to intervalley phonons, one also generally expects *two* bosonic modes at different energies to show up in $g(V)$: their relative weights provide an estimate of the relative importance of carrier-exciton vis-à-vis carrier-phonon coupling.

Further support for our view arises when we compare the DMFT optical conductivity, $\sigma_{xx}(\omega)$ in Fig. 4 as a function of T with published data⁵. Since we have kept only the two lowest bands crossing E_F from the SK fit, we do not expect accord at higher energies, but can readily make a comparison for the relevant energy range (few hundred milli-eV) of interest. Specifically, up to about 100 meV, our result matches quite well with data, including (i) the plasmon edge, (ii) the detailed optical lineshape as a function of energy up to about 100 meV, (iii) sizable optical spectral weight transfer upon raising T . The plasmon-like features are clearly visible on both regular and log-log plots as a clear absorption onset at $\simeq 15$ meV at low $T = 10$ K. Interestingly, it is also *preceded* by a ‘prepeak’ structure, centered at $\simeq 10$ meV, in

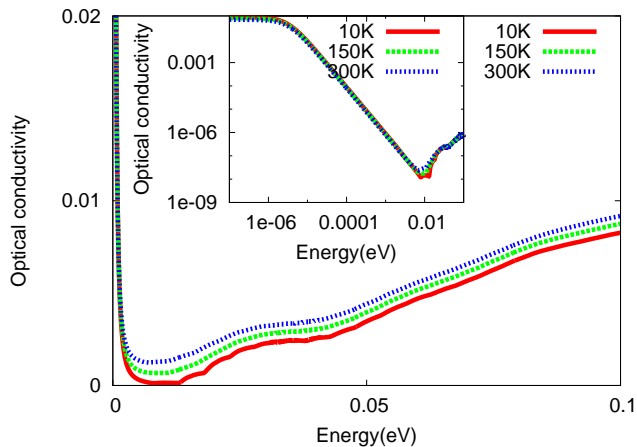


FIG. 4. (Color Online) TB+DMFT Optical Conductivity in the normal state for *Bi*. A tiny Drude-like contribution is followed by inter-band absorption: this feature onsets at $\simeq 15$ meV and originates from strong resonant scattering between the tiny number of carriers and interband excitons in DMFT. The pre-peak in the absorption, centered at $\simeq 10$ meV, also originates from the same mechanism. The inset reveals the same features in more detail on a log-log plot. These findings are in very good accord with data⁵

good accord with observations. This prepeak feature is also washed out with increasing T , in accord with data. Clear spectral weight transfer up to $\simeq 200$ meV is also found: given the tiny E_F in *Bi*, this is quite a large energy scale, attesting to considerable dynamical correlations. Finally, we find an isosbestic point around 5.0 meV as a function of T , which is another characteristic signature of dynamical electronic correlations that could be tested in extant work.

Taken together, our results strongly support the idea that a common underlying scattering process involving tiny number of carriers and uncondensed fluctuating interband excitons may be operative in *Bi*. That the dominant interaction in *Bi* has a short-range excitonic character is well known⁵. Our results show that it seems to be a sufficient *minimal* input to understand transport in *Bi*, and ties in our view with plasmarons⁴). Generally, mid-infra-red features in correlated metals (*e.g.*, DMFT for one-band Hubbard type models) involve interband transitions between low-energy itinerant and high-energy localized states. In our case, they arise from transitions involving carrier states scattering off the incoherent and interband excitons involving precisely the renormalized VB and CB, since $\sigma_{xx}(\omega)$ in DMFT is just a direct convolution of the one-particle DMFT spectral functions. In *Bi*, this feature occurs at a very low energy because of the tiny E_F . The interband electronic excitations involving carriers coupled to such exciton-like entities have been christened *plasmaron* in prior work. We find that this characterization is not in conflict with our excitonic fluctuation picture, since we have now shown that it can be well described by analyzing effects of predominantly

local and sizable excitonic liquid-like correlations in a quasi-realistic model for *Bi*.

Buoyed by the agreement with the phenomenology so far, we venture to propose a specific model for superconductivity in *Bi*. To do so, we need to generate an effective pairing interaction arising from excitonic and/or phonon fluctuation exchange. Given the efficacy of the excitonic liquid view above for the normal state, and that the exciton formation energy scale ($\Omega_{ex} \simeq \Delta_{exc}$) is quite large, we are clearly in the non-adiabatic limit. This precludes a BCS-like instability to SC in *Bi*. In the normal state, the interband excitons involving the VB and CB form an isospin $\mathbf{T} = 1/2$ degree of freedom, described by $T^+ = \sum_{k,\sigma} a_{k\sigma}^\dagger b_{k\sigma}$, $T^- = \sum_{\sigma} b_{k\sigma}^\dagger a_{k\sigma}$, $T^z = \sum_k (n_{ka} - n_{kb})/2$ in particle-hole space. Precisely as in the $U < 0$ Anderson lattice¹⁶, one has a crossover to an incoherent exciton fluctuation dominated regime at $k_B T \simeq O(U')$, followed by a second crossover to a quasi-coherent exciton fluctuation dominated regime at a lower exciton-Kondo scale, $T_K^{ex} \simeq U'(\pi J \rho)^{1/2} e^{-1/(2J\rho)}$, where $\rho = \rho(E_F)$ is the LDOS at E_F and $J \simeq t_{12}^2 \chi_{12}(0)$, with $\chi_{12}(0)$ the excitonic susceptibility at $\omega = E_F (= 0)$: correlated FL behavior obtains below T_K^{ex} , thanks to an excitonic Kondo screening implicit in a situation where a tiny number of carriers are now coupled to fluctuating isospins \mathbf{T} . It is precisely this resonant scattering that governs transport in the normal state in good accord with transport data as found above.

As T is lowered, intersite, residual interactions develop in full analogy with the Kondo lattice. They correspond to exchange coupling between isospins, and can be viewed as an exciton fluctuation-exchange process. The residual interactions read

$$H_{eff}^{(2)} \simeq J \sum_{\langle i,j \rangle, \sigma, \sigma'} a_{i\sigma}^\dagger b_{j\sigma} b_{j\sigma'}^\dagger a_{i\sigma'} \quad (3)$$

which is also $J \sum_{\langle i,j \rangle, \sigma, \sigma'} [n_{ia\sigma} - a_{i\sigma}^\dagger b_{j,-\sigma}^\dagger b_{j\sigma} a_{i,-\sigma}]$. Absorbing the first term in the normal state Hamiltonian, $H_{res}^{(2)}$ in momentum space is

$$H_{res}^{(2)} = -J \sum_{kpq} (a_{k\sigma}^\dagger b_{p,-\sigma}^\dagger b_{k-q,\sigma} a_{p+q,-\sigma} - a_{k\sigma}^\dagger b_{p,-\sigma}^\dagger b_{k-q,-\sigma} a_{p+q,\sigma})$$

Use of a usual BCS-like argument to derive SC from a static Hartree-Fock decoupling of $H_{res}^{(2)}$ is possible¹⁷, but problematic. This is because, as it stands, the effective interaction leads to possibility of both p-p and p-h condensation, and at intermediate-to-strong "excitonic Kondo" coupling, it is known that there is strong interference between both these channels at two-particle level. Then the associated logarithmic divergences appear in both channels, best illustrated within the classic parquet approach¹⁸. We have adapted Abrikosov's original parquet approach to our case (see SI for details). We proceed as follows: the bare vertex, $\Gamma_{\sigma_1 \sigma_2 \sigma_3 \sigma_4}^{(0)}(p_1, p_2, p_3, p_4) = J(\delta_{\sigma_1 \sigma_3} \delta_{\sigma_2 \sigma_4} - \delta_{\sigma_1 \sigma_4} \delta_{\sigma_2 \sigma_3})$ will obtain drastic renormalization in the 'excitonic Kondo' regime. To this end, we

exploit DMFT results: since the a -band spectral function is gapped, one can replace $G_{aa}^{-1}(\omega) \simeq \omega + \epsilon_a$ at low energy (since $\text{Im}\Sigma_{aa}(\omega) = 0$ at low energy), while the b -band propagator is approximated as $G_{bb}^{-1}(k, \omega) \simeq \omega - z_b \epsilon_{k,b}$, with $z_b^{-1} = 1 - (d/d\omega)\text{Re}\Sigma_{bb}(\omega)|_{\omega=E_F}$. With these inputs, we find that the vertex is logarithmically enhanced, giving $\Gamma(\omega) = J[1 + \rho \ln(E_F/|\omega| + \epsilon_a)]^{-1}$. The SC transition temperature is estimated from the divergence of the renormalized vertex, and we find $T_c = E_F \cdot e^{-1/J\rho}$. Using the *renormalized* $E_F \simeq T_K \simeq 100$ K from DMFT results below which correlated FL behavior sets in (instead of the *bare* $E_F \simeq 23$ meV in Bi), $\rho(E_F) \simeq 0.1\text{eV}^{-1}$ from normal state DMFT results, and the coupling $J \simeq O(1)$ (we are *not* in the regime $t_{11,22,12} \ll U'$ for Bi), we estimate the SC $T_c \simeq O(1)$ mK, quite close to the experimental finding of $T_c \simeq 0.5$ mK. Given the approximations made above, this is very reasonable. Our estimate is a huge enhancement compared to the $T_c^{BCS} \simeq O(100)$ nK found using the naive BCS formula³, and reflects the strong coupling nature of SC, where non-adiabatic effects enhance T_c via huge enhancement of the vertex. Effects akin to the above have been discussed in the non-adiabatic limit of strong electron-phonon coupling¹⁹ and, in Bi , the fact that $g/E_F \simeq O(0.5)$ will also imply such additional enhancement arising from electron-phonon coupling. In the non-adiabatic limit, it is possible to subsume this latter effect into a renormalized value of the bare vertex J and, in fact, our DMFT results do include the renormalization caused by e-p coupling as well. Such strong coupling multi-band SC will also generally give an enhanced (dH_{c2}/dT) in Bi ³, as in other documented near semi-metallic superconductors²⁰, relative to the BCS prediction.

Finally, the form of the effective interaction also shows that the excitonic insulator (EI) phase is a subleading instability in Bi . It is of interest to inquire whether evidence for such a ‘‘competing order’’ could obtain in Bi by modification of its electronic structure, *e.g.* by pressure¹ or an external magnetic field. Both reduce the tiny carrier density further, jacking up the effective U/t ratio and inducing tendency to localization. Actually, pressure does induce a metal-insulator-like transition in Bismuth¹. Within our strong coupling analysis, the competing order in the resultant semi-conducting phase would be characterized by an order parameter $\Delta_{e_x} = \sum_{k,\sigma} \langle f_{12}(k) c_{1k\sigma}^\dagger c_{2k\sigma} \rangle$ with $f_{12}(k) = 2\sqrt{3}\sin(\sqrt{3}k_x a/2)\sin(k_y a/2)$. This excitonic order parameter does not break inversion symmetry ($\mathbf{k} \rightarrow -\mathbf{k}$) but, remarkably, is associated with an electronic *nematic* order¹⁶. Very recent work²¹ finds a nematic electronic state with a tiny gap $O(500)\mu\text{eV}$ on the surface of Bi under high magnetic fields. Whether a Rashba-SOC modified electronic structure as above can induce an excitonic instability as proposed here, and whether such a state can lead to a reconstructed electronic structure having the observed anisotropy of Landau level wave-functions, is an enticing open issue. Thus, future studies under pressure can confirm or refute our prediction which, at this

time seems to have limited confirmation²¹. Investigation into these aspects is left for future work.

Supplementary Information Here, we adapt the parquet approach of Bychkov *et al.*¹⁸ to our model. In the parquet approach¹⁸, graphs corresponding to p-h and p-p vertices which cannot be cut into two separate pieces by cutting two (a , the ‘‘heavy’’ band, or b , the metallic band in Bi) propagator lines are neglected. However, the leading logarithmic corrections arising from Kondo screening are retained. At N th order, the magnitude of each diagram for Γ is x^N , where $x = J\rho \int G_{aa}G_{bb}d\omega d\epsilon \simeq J\rho \ln(E_F/|\omega| + \epsilon_a) \simeq O(1)$. The full vertex in the parquet approximation is $\Gamma = \Gamma_0 + \Lambda_{pp} + \Lambda_{ph}$, with Γ_0 the bare vertex, Λ_{pp} the p-p ‘‘brick’’ which can be cut by two parallel a, b propagator lines, and Λ_{ph} the corresponding brick in the p-h channel. The parquet series is analyzed by requiring (i) no energy transfer to and from the internal (gapped) a -band (gapped in case of Bi , see DMFT results) states; thus, one can set $\omega_2 = \omega_3 = 0$ and $\omega_1 = \omega_4 = \omega$, (ii) all momenta $p_i, i = 1, 2, 3, 4$ are set equal to p_F . (iii) using $\Gamma(\omega, 0, 0, \omega) = \Gamma(\omega)$, and choosing an *internal* two-line state such that the energy ω' of the G_{aa} line is minimum. Since there is a *full* vertex part $\Gamma(\omega')$ to the left and right of this part, one finds¹⁸,

$$\Gamma_{\sigma_i}^P(\omega) = \rho \int_{|\omega|}^{E_F} \frac{\Gamma_{\sigma_1\sigma_4\mu\nu}(\omega')\Gamma_{\mu\nu\sigma_2\sigma_3}(\omega')}{\omega'} d\omega' \quad (4)$$

and

$$\Gamma_{\sigma_i}(\omega) = \rho \int_{|\omega|}^{E_F} \frac{\Gamma_{\sigma_1\nu\mu\sigma_4}(\omega')\Gamma_{\mu\sigma_2\sigma_3\nu}(\omega')}{\omega'} d\omega' \quad (5)$$

Using the spin-separable structure of Γ , one obtains $\Gamma(x) = J - J\rho \int_0^x \Gamma^2(x')dx'$, with $x = \ln(E_F/|\omega| + \epsilon_a)$. This has the solution $\Gamma(\omega) = J[1 + \rho \ln(E_F/|\omega| + \epsilon_a)]^{-1}$, showing up the logarithmic enhancement of the two-particle vertex. Hence, with $J > 0$ (notice that this co-efficient of $H_{res}^{(2)}$ is *negative* as above), $\Gamma(\omega)$ has a pole when $\Gamma^{-1}(\omega_c = T_c) = 0$, signalling an instability to the superconducting state when $T_c \simeq E_F \cdot e^{-1/J\rho}$. Thus, this enhancement of T_c relative to the simple weak-coupling BCS estimate is a consequence of the logarithmic enhancement of the vertex function. Using the *renormalized* $E_F \simeq T_K \simeq 100$ K from DMFT results below which correlated FL behavior sets in (instead of the *bare* $E_F \simeq 23$ meV in Bi), $\rho(E_F) \simeq 0.1\text{eV}^{-1}$, and the coupling $J \simeq O(1)$ (we are *not* in the regime $t_{11,22,12} \ll U'$ for Bi), we estimate the SC $T_c \simeq O(1)$ mK, quite close to the experimental finding of $T_c \simeq 0.5$ mK.

The above parquet analysis also suggests that T_c could be enhanced further if it would be possible to move the a -band states (ϵ_a) closer to the Fermi energy by appropriate perturbations.

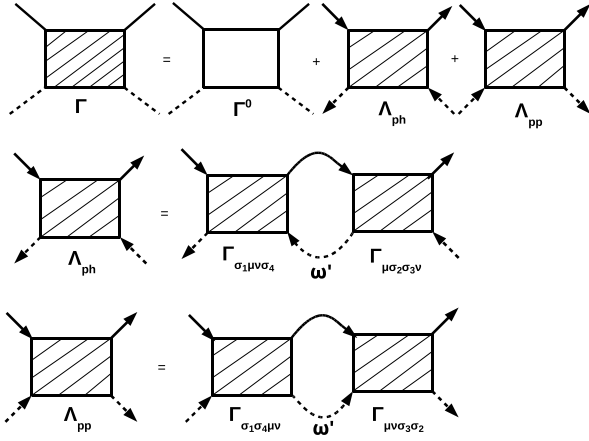


FIG. 5. The diagrammatic representation of the parquet approximation for the full vertex function (upper figure) and the blocks in the particle-hole (ph, center figure) and particle-particle (pp, lower figure) channels (see text for details).

- * sudiptakoley20@gmail.com
† msaad@imsc.res.in
‡ arghya@phy.iitkgp.ernet.in
- ¹ N. P. Armitage, R. Tediosi, F. Lévy, E. Giannini, L. Forro, and D. vander Marel, *Phys. Rev. Lett.* **104**, 237401 (2010).
 - ² K. Behnia, L. Balicas, and Y. Kopelevich, *Science* **317**, 1729 (2007).
 - ³ Om Prakash, A. Kumar, A. Thamizhavel and S. Ramakrishnan, arXiv:1603.04310, to appear in *Science*.
 - ⁴ P. Chudzinskii and T. Giamarchi, *Phys. Rev. B* **84**, 125105 (2011).
 - ⁵ R. Tediosi, N. Armitage, E. Giannini, and D. vander Marel, *Phys. Rev. Lett.* **99**, 016406 (2007).
 - ⁶ J. H. Xu, E. G. Wang, C. S. Ting, and W. P. Su, *Phys. Rev. B* **48**, 17271 (1993).
 - ⁷ M. L. Cohen, *Phys. Rev.* **134**, A511 (1964).
 - ⁸ A. Taraphder, S. Koley, N. S. Vidhyadhiraja and M. S. Laad, *Phys. Rev. Lett.* **106**, 236405 (2011).
 - ⁹ C. A. Kukkonen and K. F. Sohn *Journal of Physics F: Metal Physics*, **7**, L193 (1977).
 - ¹⁰ S. Koley, M. S. Laad, N. S. Vidhyadhiraja and A. Taraphder, *Phys. Rev. B* **90**, 115146 (2014); S. Koley, N. Mohanta and A. Taraphder, *J. Phys. Condens. Matter* **27** 185601 (2015).
 - ¹¹ N. Dasari, W. R. Mondal, P. Zhang, J. Moreno, M. Jarrell and N. Vidhyadhiraja, *Eur. Phys. Journal B*, (in press) (2016).
 - ¹² M. Keller, W. Metzner, and U. Schollwck, *Phys. Rev. Lett.* **86**, 4612 (2001).
 - ¹³ S. S. Kancharla and S. Okamoto, *Phys. Rev. B* **75**, 193103 (2007).
 - ¹⁴ S. D. Das, M. S. Laad, L. Craco, J. Gillett, V. Tripathi, and S. E. Sebastian, *Phys. Rev. B* **92**, 155112 (2015); L. de' Medici, S.R. Hassan, M. Capone, Xi Dai, *Phys. Rev. Lett.* **102**, 126401 (2009).
 - ¹⁵ J. Tomczak and S. Biermann, *Phys. Rev. B* **80**, 085117 (2009).
 - ¹⁶ A. Taraphder and P. Coleman, *Phys. Rev. Lett.* **66**, 2814 (1991).
 - ¹⁷ S. Koley, arXiv:1606.02841.
 - ¹⁸ Yu. Bychkov, L. Gorkov and I. Dzyaloshinskii, *J. Exptl. Theor. Phys. (U.S.S.R)* **50**, 738 (1966); K. Svozil, *Physica Status Solidi*, **147**, 635 (1988).
 - ¹⁹ L. Pietronero and S. Straessler, *Europhys. Lett.* **18**, 627 (1992).
 - ²⁰ DJ Singh, *PLoS ONE* **10**, e0123667 (2015).
 - ²¹ Benjamin E. Feldman, Mallika T. Randeria, Andrs Gyenis, Fengcheng Wu, Huiwen Ji, R. J. Cava, Allan H. MacDonald, Ali Yazdani, arXiv:1610.07613 (2016).